In: Geothermal Energy, Technology and Geology
Editor: Jianwen Yang
ISBN: 978-1-61942-765-5

Chapter 8

PERFORMANCE ANALYSIS OF SINGLE-FLASH GEOTHERMAL POWER PLANTS: GAS REMOVAL SYSTEMS POINT OF VIEW

Nurdan Yıldırım Ozcan[1] and Gulden Gokcen[1,2,1]

[1] Mechanical Engineering Department, Izmir Institute of Technology, Urla, Izmir, Turkey
[2] Center for Geothermal Research, Izmir Institute of Technology, Urla, Izmir, Turkey

NOMENCLATURE

AS: Air-steam ratio (-).
C_p: Constant pressure specific heat (kJ/kg K).
$C_{v:}$ Constant volume specific heat (kJ/kg K).
Ex: Exergy (kW).
f: Noncondensable gas fraction (weight % of steam).
h: Enthalpy (kJ/kg).
I: Exergy loss (kW).
M: Molar mass (kg/kmol).
$\dot{m}$: Mass flowrate (kg/s).
P: Pressure (kPa).
Ru: Universal gas constant, 8.314 kJ/(kmol K).
T: Temperature (K).
TAE: Total air equivalent (kg/s).
$\dot{W}$: Power (kW).
x: Quality (-).

[1] E-mail: *guldengokcen@iyte.edu.tr*.

Greek Symbols

η: Efficiency (-).
$\dot{\upsilon}$: Volume flowrate (m^3/s).
ΔP: Pressure drop (Pa).
γ: The ratio of the C_{pCO2}/C_{vCO2} (-).
ω : Humidity ratio (-).

Subscripts

A: Dry air.
ac: After-condenser.
air, A: Air inlet.
air, B: Air outlet.
aux: Auxiliary.
comp: Compressor.
cond: Condenser
CO_2: Carbon dioxide.
ct: Cooling tower.
cw: Cooling water.
d: Discharge.
dem: Demister.
ex: Exergy.
fan(s): Fan(s).
gc: Gas cooler.
gen : Generator.
grs: Gas removal system.
hot,air: Hot air.
i: Indice for steam jet ejectors.
ic: Inter-condenser.
in: Inlet.
is: Isentropic.
liq: Liquid.
motor, pump: Motor pump.
motor,fan: Motor fan.
NCG: Non-condensable Gas.
net: Net.
Out: Outlet.
Overall: Overall.
pump(s): Pump(s).
s: Suction.
st: Steam.
sep: Separator.
sje: Steam jet ejector.

tur: Turbine.
tur-gen: Turbine-generator.
total: Total.
wb: Wet bulb.

Abbreviations

CS: Compressor System.
GPP: Geothermal Power Plant.
HPC: High pressure compressor.
HS: Hibrid System.
LPC: Low pressure compressor.
LRVP: Liquid ring vacuum pump.
NCG: Non-Condensable Gas.
RS: Reboiler System.
SJES: Steam Jet Ejector System.

ABSTRACT

Non-condensable gases (NCGs), natural components of geothermal fluids, affect the performance of a geothermal power plant (GPP) significantly. Therefore, the NCGs should be removed from the process to optimise the thermodynamic efficiency of the plant. GPPs require large capacity NCG removal systems that occupy large portion in the total plant cost and auxiliary power consumption. The flashed-steam GPPs, which are commonly used in the World, are a relatively simple way to convert geothermal energy into electricity when the geothermal wells produce a mixture of steam and liquid. The primary aim of this study is to develop a code for simulating flashed-steam GPPs to examine the thermodynamic performance of NCG removal systems, which represent major concerns at planning and basic design stages of GPPs. A single-flash GPP model is developed and simulated to identify the effects of input variables, such as NCG fraction, separator pressure and condenser pressure. Among the variables, NCG fraction is the most significant parameter affecting thermodynamic performance of single-flash GPPs. The net power output and overall exergetic efficiency of single-flash GPP are decreased 0.4% for compressor system (CS), 2.2% for hybrid system (HS), 2.5% for reboiler system (RS), and 2.7% for steam jet ejector system (SJES) by 1% increase in NCG fraction.

1. INTRODUCTION

In flashed-steam geothermal power plants (GPPs), steam used for power generation is not pure but contains non-condensable gases (NCGs) (CO_2, H_2S, NH_3, N_2, CH_4 etc.). The NCGs are the natural components of geothermal fluids. The amount of NCGs contained in geothermal steam has significant impact on power generation performance of a GPP. Depending on the resource, the fraction of the NCGs can vary from less than 0.2% to greater than 25% by weight of steam [1,2].

The practical problems caused by elevated levels of NCGs in geothermal power plants are:

- The gases reduce the heat transfer efficiency of the condensers by increasing the condenser operating pressure, which reduces turbine power output;
- NCGs contain lower recoverable specific energy than steam does;
- Higher capital and operating cost for gas removal in the cost of electricity than fossil-fuelled power plants, and;
- Acid gases such as carbon dioxide and hydrogen sulphide are highly water-soluble and contribute to corrosion problems in piping and equipment that contact steam and condensate [3].

Systems and processes that degrade the quality of energy resources can only be identified through a detailed thermodynamic analysis of the whole system. Most cases of thermodynamic imperfection cannot be detected by an energy balance. A careful evaluation of processes using exergy balance enables the identification of the source of inefficiencies and waste, which leads to improved designs and resultant savings. Exergy analysis is a technique that uses the conservation of mass and energy principles together with the second law of thermodynamics [4]. Efficiencies that are a measure of an approach to the ideal case can be evaluated, and the process steps having the largest losses can be identified by exergy analysis [5, 6].

The influence of NCGs on the performance of GPPs was first studied by Khalifa and Michaelides [7]. The authors reported that the presence of 10% NCG in the geothermal steam results in as much as a 25% decrease in the net work output compared to a clean steam system. Michaelides [8] proposed a flash system at the wellhead to separate the NCGs before they enter the turbine and determined the flash temperature depending on the NCG content. It is emphasised that NCG content in the steam is an important factor for the estimation of the recoverable work. If NCG content is higher than 0.1%, separating the NCGs by flashing at the wellhead results in a higher amount of work recovery. It is recommended that if NCG content is high, NCG removal should be taken into account thermodynamically and economically for the construction of plants. To increase power generation performance, upstream reboiler systems are investigated as an alternative to conventional gas extraction systems [2, 9-10] and applied in Italy on a commercial scale [11, 12].

Yildirim and Gokcen [13] considered the NCG content on each step of energy and exergy analysis of Kizildere Geothermal Power Plant. They emphasised the importance of NCGs on power plant performance and concluded that since geothermal power plants contain a considerable amount of NCGs, the NCG content should not be omitted throughout the process and dead state properties should reflect the specified state properties.

The studies reveal that the presence of NCGs in geothermal steam results in a dramatic decrease in the net work output compared to clean steam. Because of the elevated NCG levels, GPPs require large capacity NCG removal systems. Therefore, selection of NCG removal system becomes a major concern at planning and basic design stages of geothermal power plants [14-15].

The conventional gas removal systems used in geothermal power plants are:

- Jet ejectors, e.g. steam jet ejectors, which are suitable for low NCG flows (<3%);
- Liquid ring vacuum pumps (LRVPs);
- Roto-dynamic, e.g. radial blowers, centrifugal compressors, which are mainly used for large NCG flows (>3%), and;
- Hybrid systems (any combination of equipment above).

The aim of this study is to model a single-flash GPP to examine the thermodynamic performance of NCG removal systems. A model is developed for various NCG removal system options, including:

- compressor system (CS);
- steam jet ejector system (SJES);
- hybrid (steam jet ejector and LRVP) system (HS), and;
- reboiler system (RS).

by employing Engineering Equation Solver (EES) software [16] that solves mass, energy and exergy balances for each plant component. The model is validated by Kizildere GPP-Turkey data. The simulation is performed on the disturbances of input parameters, including geothermal field (e.g., NCG fraction, and separator pressure) and plant (e.g., condenser pressure, and turbine inlet temperature) parameters.

2. Overview of the System

Figure 1 shows a schematic diagram of a representative single-flash GPP model. The plant mainly consists of production wells, wellhead/main separator(s), turbine, condenser, NCG removal system, cooling tower, and auxiliary equipment such as pumps and fans. Geothermal fluid, which is a mixture of liquid, water vapor and NCGs at the wellhead, is separated into the steam and liquid phases at the separator. Steam phase directed to the turbine contains water vapor and NCGs. After passing the turbine, steam, condensate and NCGs flow to the condenser where NCGs are accumulated and extracted by a gas removal system. The rest is pumped to the cooling tower which helps the temperature of the fluid drops down to the cooling water temperature to be re-used in the condenser. Liquid phase is driven by circulation pumps and air is drawn into the cooling tower by fans.

3. Methodology

The plant is first modelled for four gas removal options using EES software, then energy and exergy analysis is carried out to evaluate the net power output of the plant under a range of NCG fraction (0-25%).

Average fluid and ambient properties are kept constant and some general assumptions are made for modelling. The constant properties are taken from Kizildere Geothermal Power Plant (KGPP)-Turkey which is a single-flash GPP and is a unique case in the World having

the highest NCG fraction as a conventional GPP. Table 1 lists the general assumptions and constant parameters which are taken from KGPP [1, 15, 17, 18-22].

Overall mass, energy and exergy balance for steady-state conditions with reference to Figure 1 can be expressed as below [23]. The subscript numbers refer to state locations in Figure 1.

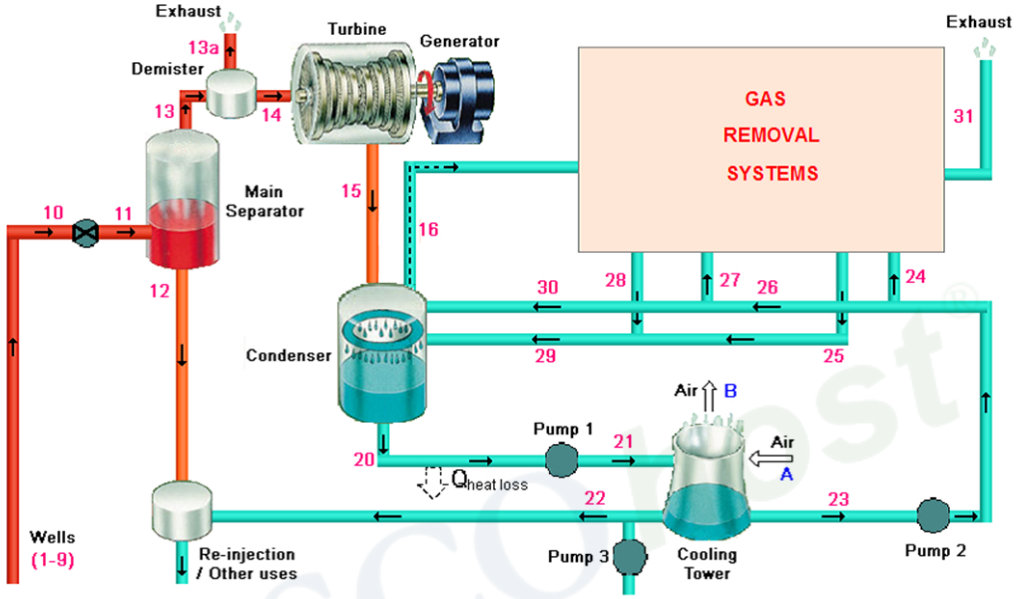

Figure 2. Schematic diagram of a representative single-flash GPP.

Table 1. Constant parameters and general assumptions [1, 15, 17, 18-22]

Constant Parameters		
Wellhead pressure	(kPa)	1426
Wellhead flowrate	(t/h)	870.1
Atmospheric pressure	(kPa)	95
Yearly average outdoor temp.	(°C)	16
Wet bulb temperature	(°C)	13
Relative humidity	(%)	65
NCG fraction in steam	(%)	13
CO_2 fraction in NCG	(%)	96-99
Condenser pressure	(kPa)	10
T_{23} (Figure1)	(°C)	29
General Assumptions		
η_{comp}	(%)	75
η_{gen}	(%)	90
T_{wb}	(°C)	13
T_{21}-$T_{hot,air}$ (Figure 1)	(°C)	6
T_{20}- T_{21} (Figure 1)	(°C)	3
P_{13}- P_{14} (Figure 1)	(kPa)	10
η_{pump}, η_{fan}	(%)	70
$\eta_{motor,pump}$, $\eta_{motor,fan}$	(%)	85
$\Delta P_{\Delta P_{pump}}$, $\Delta P_{\Delta P_{fan}}$	(kPa)	100

Constant Parameters		
P_{19}	(kPa)	105
T_{CO2}	(°C)	T_{wb}
P_{16} (Figure 1)	(kPa)	$0.90P_{cond}$

Geothermal fluid at the wellhead is saturated vapour-liquid mixture.
CO_2 is an ideal gas and not dissolved in the water.
Baumann Rule applies to turbine efficiency $\eta_{t..}$
At the turbine exit isentropic quality calculations consider NCGs.
Pressure ratios are equal at gas removal system stages.

$$\dot{m}_{10} + \dot{m}_{air_A} = \dot{m}_{12} + \dot{m}_{13a} + \dot{m}_{22} + \dot{m}_{31} + \dot{m}_{air_B} \tag{1}$$

$$\dot{W}_{net} = \dot{W}_{gen} - \sum \dot{W}_{aux} \tag{2}$$

$$\dot{W}_{aux} = \sum \dot{W}_{grs} + \dot{W}_{motor,pump} + \dot{W}_{motor,fan} + \dot{W}_{other} \tag{3}$$

$$\dot{E}x_{10} + \dot{E}x_{air,A} = \dot{E}x_{12} + \dot{E}x_{13a} + \dot{E}x_{22} + \dot{E}x_{heatloss,pipe} + \dot{E}x_{31} + \dot{E}x_{air,B} + \dot{W}_{net} + \sum I_{GPP} \tag{4}$$

where

$\dot{E}x_{heatloss\ ,pipe}$: Exergy loss through pipe between condenser exit and cooling tower inlet,

$\sum I_{GPP}$: Total exergy destruction.

The overall exergetic efficiency of the plant is expressed as:

$$\eta_{overall} = \frac{\dot{W}_{net}}{\dot{E}x_{10}} \tag{5}$$

The GPP is simplified into several sub-systems, each with distinct mass, energy and exergy inflows and outflows and being approximated into steady-state flow. In the following section, the mass, energy and exergy balance equations for all the plant components (including separator, demister, turbine-generator, condenser, cooling tower, NCG removal system, and auxiliary equipment such as fans and pumps) are introduced.

3.1. Separator

The geothermal fluid is separated into vapor and liquid in a steam separator (Figures 2 and 3). As illustrated in Figure 2, the sequence of processes begins with geothermal fluid under pressure at state 10 (also see Figure 1) close to the saturation curve.

The flashing process in the well is modelled as an isenthalpic process, because it occurs steadily, spontaneously, essentially adiabatically, and with no work involvement. Any change in the kinetic or potential energy of the fluid is also neglected. Thus it can be written as:

$$h_{11} = h_{10} \tag{6}$$

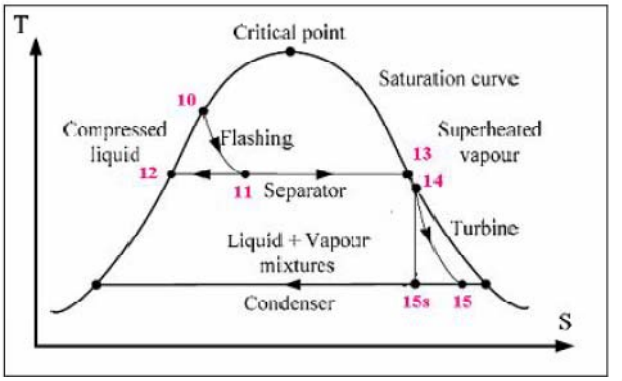

Figure 3. T-s diagram for a single-flash plant [24].

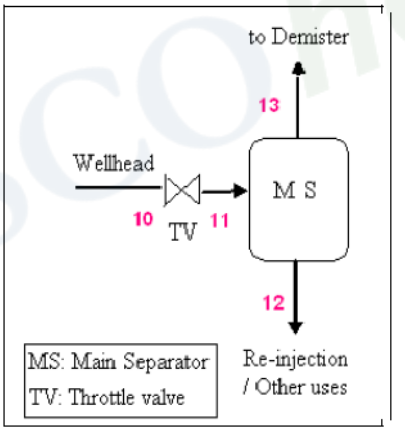

Figure 4. Main separator flow process.

The separation process is an isobaric process, once the flash has taken place. That is

$$P_{11} = P_{12} = P_{13} = P_{sep} \tag{7}$$

The quality of dryness fraction, x, of the mixture that forms after the flash, state 11, can be found from:

$$x_{11} = \frac{h_{11} - h_{12}}{h_{13} - h_{12}} \tag{8}$$

The mass flowrate of steam that flows to the turbine from the separator is given by:

$$\dot{m}_{13} = x_{11}\dot{m}_{11} \tag{9}$$

Then, the mass flowrate of the brine from the separator is written as:

$$\dot{m}_{12} = (1 - x_{11}) \times \dot{m}_{11} \tag{10}$$

Exergy loss and exergetic efficiency are of the form:

$$I_{sep} = \dot{E}x_{10} - \dot{E}x_{12} + \dot{E}x_{13} \tag{11}$$

$$\eta_{Ex\,sep} = \frac{\dot{E}x_{13}}{\dot{E}x_{10}} \tag{12}$$

3.2. Demister

A demister, shown in Figure 4, is employed to remove the condensate from the steam and make sure dry steam is introduced to the turbine. The pressure drop through the demister is taken as 10 kPa and the flashed mass flowrate is considered as 1% of the steam flowrate [18].

$$\dot{m}_{13a} = 0.01 \times \dot{m}_{13} \tag{13}$$

Exergy loss and exergetic efficiency are of the form:

$$I_{dem} = \dot{E}x_{13} - \dot{E}x_{14} - \dot{E}x_{13a} \tag{14}$$

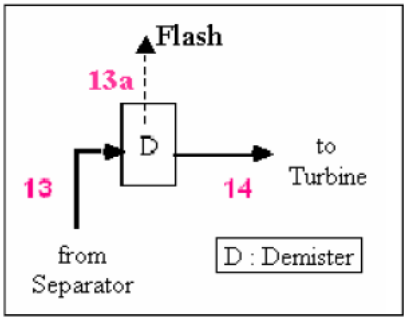

Figure 5. Flow diagram of demister.

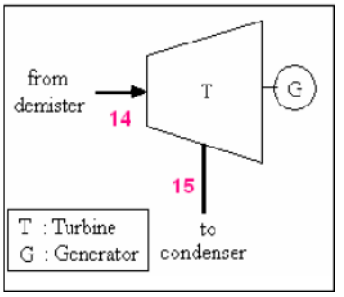

Figure 6. Turbine expansion flow process.

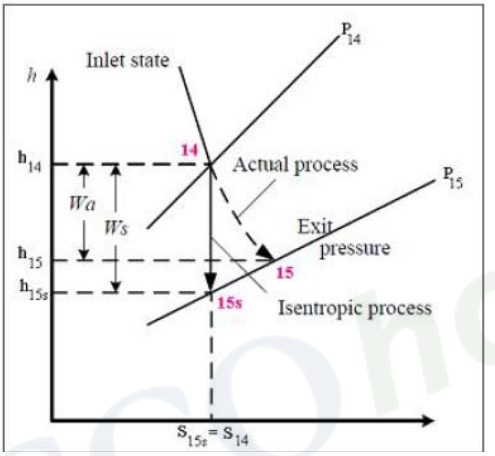

Figure 7. h-s diagram for the actual and isentropic processes of an adiabatic turbine

$$\eta_{Ex,dem} = \frac{\dot{E}x_{14}}{\dot{E}x_{13}} \tag{15}$$

3.3. Steam Turbine and Generator

Turbine expansion process is illustrated in Figure 5. For a turbine under steady operation, the inlet state of the working fluid and the exhaust pressure are fixed. Therefore, the ideal process for an adiabatic turbine is an isentropic process between the inlet state and the exhaust pressure (Figure 6).

Turbine power is given by the following equation:

$$\dot{W}_{tur} = \dot{m}_{14} \times (h_{14} - h_{15}) \tag{16}$$

The turbine isentropic efficiency (η_{tur}) is given by:

$$\eta_{tur} = \frac{\text{Actual turbine work}}{\text{Isentropic turbine work}} = \frac{\dot{W}_{tur}}{\dot{W}_{tur,is}} \tag{17}$$

Usually the changes in kinetic and potential energies, associated with a fluid stream flowing through a turbine, are small compared to the change in enthalpy, and hence can be neglected. The work output of an adiabatic turbine therefore simply becomes the change in enthalpy, and the equation becomes [18]:

$$\eta_{tur} = \frac{h_{14} - h_{15}}{h_{14} - h_{15,is}} \tag{18}$$

Steam turbine efficiencies are calculated by a modified Baumann rule [20];

$$\eta_{tur} = 0.85 \times (1 - 1.2 \times (1 - x_{15,is})) \tag{19}$$

To determine the steam turbine efficiency, it is necessary to calculate the isentropic quality ($_{x15,is}$) at the turbine exit:

$$x_{15,is} = \frac{s_{15,is} - s_{l,15}}{s_{15} - s_{l,15}} \tag{20}$$

The actual turbine power is calculated using the actual enthalpy of the geothermal fluid at state 15 by using Eq. 18. Thus, the turbine power is calculated by Eq. 16. The turbine-generator power is defined by the following equation:

$$\dot{W}_{gen} = \dot{W}_{tur} \times \eta_{gen} \tag{21}$$

Exergy loss and exergetic efficiency:

$$I_{tur-gen} = \dot{E}x_{14} - \dot{E}x_{15} - \dot{W}_{tur} \tag{22}$$

$$\eta_{Ex_{tur-gen}} = \frac{\dot{W}_{tur}}{\dot{E}x_{14} - \dot{E}x_{15}} \tag{23}$$

3.4. Condenser

The primary purpose of the condenser is to condense the exhaust steam leaving the turbine. The circulating water system supplies cooling water to the turbine condensers and

thus acts as a vehicle by which heat is rejected from the steam cycle to the environment. Its performance is vital to the efficiency of the power plant itself because a condenser operating at a lowest temperature will result in maximum turbine work and cycle efficiency with a minimum heat rejection. The typical condensate temperature attained in practice is 45-50°C, corresponding to a condenser pressure of 9.6-12.5 kPa-abs [26-26].

Figure 7 presents the temperature distribution in a condenser. The circulating-water inlet temperature should be sufficiently lower than the steam-saturation temperature to produce reasonable values of ΔT_0. It is usually recommended that ΔT_i should be between about 11 and 17°C and that ΔT_0, should not be less than 2.8°C. The enthalpy drop and turbine work per unit pressure drop are much greater at the low-pressure end than at the high-pressure end of a turbine [25].

There exist two types of condensers: direct contact and surface condensers. The most common type used in GPPs is direct-contact condensers [17]. The flow diagram of a direct-contact condenser is shown in Figure 8. Steam leaving the turbine (15) is exhausted into the condenser where it is mixed with a spray of cold water from the cooling tower (30) and gas coolers of the NCG removal system (29). The steam condenses as water droplets and the condensate drains through a barometric leg (20) into a seal pit tank to overcome atmospheric pressure. NCGs and a small amount of steam are sucked from the condenser (16) by NCG removal system.

The condenser heat load can be calculated using the following equation:

$$\dot{Q}_{con} = \dot{m}_{15} \times h_{15} - \dot{m}_{16} \times h_{16} - \left[\dot{m}_{l,15} + (\dot{m}_{s,15} - \dot{m}_{s,16})\right] \times h_{20} \tag{24}$$

The cooling water mass flowrate is calculated as:

$$\dot{m}_{30} = (\dot{Q}_{con} - \dot{m}_{29} \times (h_{20} - h_{29})) / (h_{20} - h_{30}) \tag{25}$$

Exergy loss and exergetic efficiency are of the form:

$$I_{con} = \dot{E}x_{15} + \dot{E}x_{29} + \dot{E}x_{30} - \dot{E}x_{16} - \dot{E}x_{20} \tag{26}$$

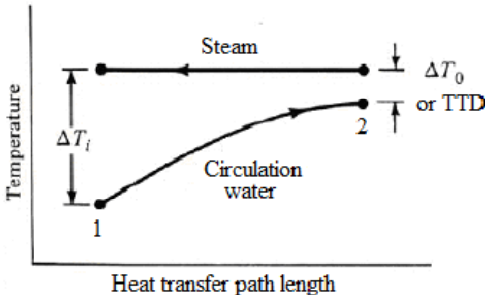

Figure 8. Condenser temperature distribution [17].

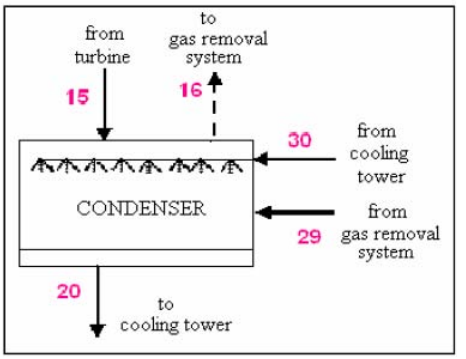

Figure 9. Condenser flow diagram.

$$\eta_{Ex,con} = \frac{\dot{E}x_{16} + \dot{E}x_{20}}{\dot{E}x_{15} + \dot{E}x_{29} + \dot{E}x_{30}} \tag{27}$$

3.5. Cooling Tower

Power plants generate large quantities of waste heat that is often discarded through cooling water in nearby lakes or rivers. In some cases, however, the cooling water supply is limited or thermal pollution is a serious concern. In such cases the waste heat must be rejected to the atmosphere, with cooling water re-circulating and serving as a transport medium for heat transport between the source and the sink (the atmosphere). One way of achieving this is through the use of cooling tower.

A cooling tower is an evaporative heat transfer device in which atmospheric air cools warm water, with direct contact between the water and the air, by evaporating part of the water [17].

The mass and energy balances between hot water and cold air entered, cold water and hot air exiting the cooling tower are shown in Figure 9.

The circulating condensate leaving (20) the condenser is pumped by a circulating water pump (Pump1) to the top of the cooling towers (21). Water reaches the top of the cooling towers with a 3°C temperature drop. As the water droplets fall down and break up into fine droplets, a stream of air (A) flows across the water droplets thus creates cooling by evaporation and convection-conduction mechanisms. The stream of air is created by suction of air fans ($\dot{W}_{fan}$) located at the top of the cooling towers. The water droplets eventually fall into the cold pond from which water is transferred into the condenser inlet pipeline (23). Some water goes to the gas cooler of the NCG removal system and the rest into the condenser. Warm moist air leaves the cooling tower (B), driven out by air fans ($\dot{W}_{fan}$). Some condensate is lost to the air. Changes in potential and kinetic energy and heat transfer are all negligible. No mechanical work is done. The dry air goes through the tower unchanged. The water vapor in the air gains mass due to the evaporated water.

Thus, based on a unit mass of dry air, and with the subscripts A and B referring to air inlet and exit and with the subscripts 21 and 23 to circulating water inlet and exit (the air

leaving the system at B is often saturated), and also following psychometric practice, the equations are written for a unit mass of dry air [25]:

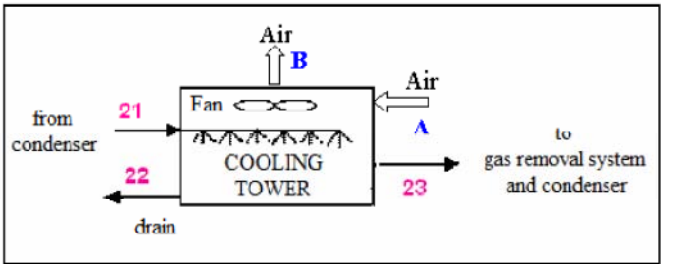

Figure 10. Cooling tower flow diagram.

$$h_{a_A} + \omega_A \div h_{s_A} + W_{21} \times h_{l_{21}} = h_{a_B} + \omega_B \times h_{s_B} + W_{23} \times h_{l_{23}} \tag{28}$$

$$\omega_B - \omega_A = W_{21} - W_{23} \tag{29}$$

From the cooling water calculation in the condenser section, it is known that the volume flowrate of hot cooling water entering the cooling tower is $\dot{m}_{cw}$ (m^3/s). Thus, dry air mass flowrate can be found:

$$\dot{m}_a = \dot{m}_{cw} / W_{21} \tag{30}$$

Exergy loss and exergetic efficiency have the form:

$$I_{ct} = \dot{E}x_{21} + \dot{E}x_{air,A} + \dot{W}_{fan} - \dot{E}x_{22} - \dot{E}x_{23} - \dot{E}x_{air,B} \tag{31}$$

$$\eta_{Ex,ct} = \frac{\dot{E}x_{21} + \dot{E}x_{air,A} - I_{ct} - \dot{E}x_{22} - \dot{E}x_{exhaust}}{\dot{E}x_{21} + \dot{E}x_{air,A}} \tag{32}$$

3.6. NCG Removal Systems

In this study detailed energy and exergy analyses are conducted for a single-flash GPP for four different types of gas removal systems, which are:

- Two-stage steam jet ejector system (SJES);
- Two-stage hybrid system (steam jet ejector and LRVP) (HS);
- Two-stage compressor system (CS), and;
- Reboiler system (RS).

3.6.1. Steam Jet Ejectors (SJES)

Steam jet ejectors remove the NCGs from the condenser and compress them to the atmospheric pressure with the expense of steam. Since an ejector has no valves, rotors, pistons or other moving parts, it is a relatively low-cost component and easy to operate. It requires relatively little maintenance but consumes a considerable amount of steam. Because the capacity of a single ejector is fixed by its dimensions, a single unit has practical limits on the total compression and throughput it can deliver. For greater compression, two or more ejectors can be arranged in series. Two-stage steam jet ejector system is shown in Figure 10.

Steam consumption of steam jet ejectors increases with increasing NCG fraction. Therefore, it is important to define the steam flowrate precisely (Eq. (33) [1].

$$\dot{m}_{33} = \frac{TAE_1}{AS_1}, \dot{m}_{34} = \frac{TAE_2}{AS_2} \tag{33}$$

The corresponding potential work of steam consumed can be calculated as in Eq. (34).

$$\dot{W}_{se} = \dot{m}_{32}.(h_{14} - h_{15}) \tag{34}$$

Exergy loss of steam jet ejectors and gas coolers is the difference between exergy input and output and calculated by Eq. (35).

$$I_{sje}, I_{gc} = \sum Ex_{in} - \sum Ex_{out} \tag{35}$$

The exergetic efficiency is the ratio of total exergy output (E_{xout}) to exergy input (E_{xin}) of the steam jet ejectors and gas coolers.

$$\eta_{ex_{sje}}, \eta_{ex_{gc}} = \frac{\sum Ex_{out}}{\sum Ex_{in}} \tag{36}$$

3.6.2. Hybrid System (Steam Jet Ejector + LRVP) (HS)

LRVP is a rotary compressor type device and is generally used alone in low flow applications where large pressure ratios are not required. It has been proposed for use for geothermal applications in series with a steam jet ejector, which provides the first stage of compression [1]. Integration of a steam jet ejector with a LRVP is commonly referred as a hybrid system. It is one of the more efficient methods for producing a process vacuum. The flow diagram of the hybrid system is shown in Figure 11.

The LRVP work is calculated by Eq. (37) [1, 17].

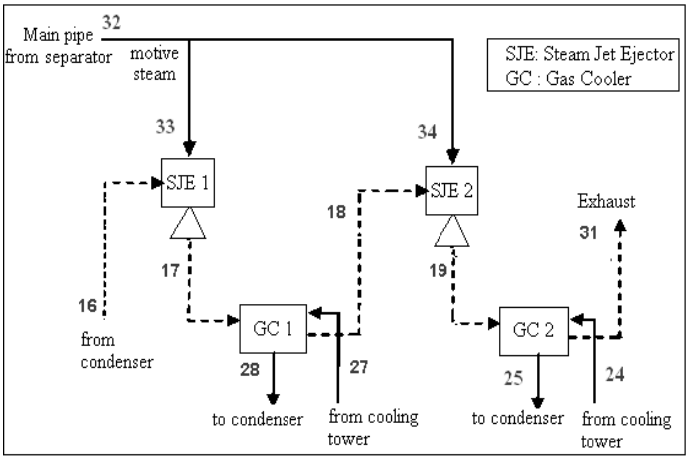

Figure 10. Flow diagram of two-stage steam jet ejector system.

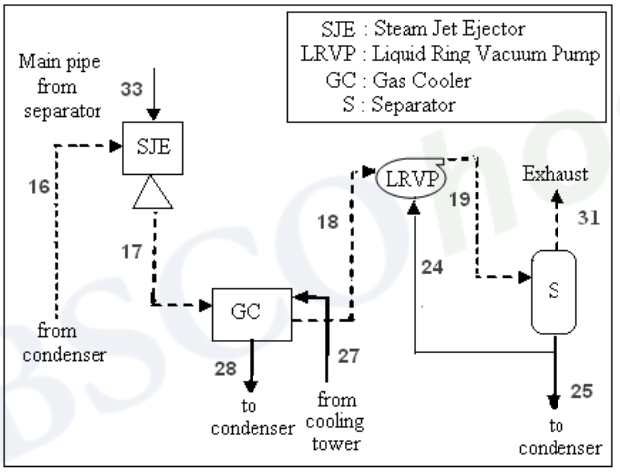

Figure 11. Flow diagram of hybrid system.

$$\dot{W}_{LRVP} = \left[\frac{\gamma}{\gamma - 1}\right] \frac{\dot{m}_{CO_2}.Ru.T_{CO_2}}{\eta_{LRVP}.M_{CO_2}} \left[\left(\frac{P_d}{P_s}\right)^{\left(1-\frac{1}{\gamma}\right)} - 1\right] \tag{37}$$

where $\dot{W}_{LRVP}$ is the liquid ring vacuum pump work.

For liquid ring vacuum pump, the exergy loss is:

$$I_{LRVP} = Ex_{18} - Ex_{19} + \dot{W}_{LRVP} \tag{38}$$

The exergetic efficiency of the liquid ring vacuum pump is calculated as:

$$\eta_{ex\,LRVP} = \frac{Ex_{19} - Ex_{18}}{\dot{W}_{LRVP}} \tag{39}$$

3.6.3. Centrifugal Compressors (CS)

Increasing NCG fraction increases steam consumption of steam jet ejectors and consequently operational cost becomes uneconomic. Centrifugal compressors, although expensive to install, have overall efficiencies in order of 75%. When dealing with large quantities of NCGs this makes them the preferred option compared to the other systems. A two-stage compressor system flow diagram is shown in Figure 12.

Power consumption of the compressors is calculated as Eq. (40).

$$\dot{W}_{comp} = \dot{m}\ .\Delta h \tag{40}$$

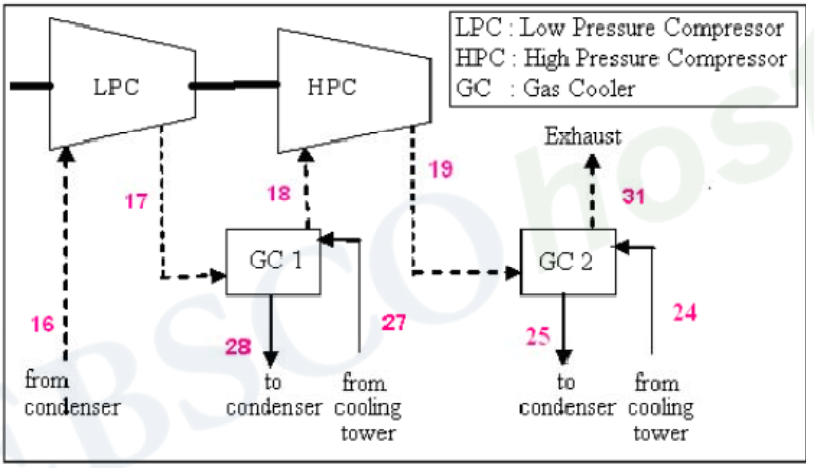

Figure 12. Flow diagram of two-stage compressor system.

Exergy loss of the compressors is calculated with reference to Figure 12 as:

$$I_{LPC} = Ex_{16} - Ex_{17} + \dot{W}_{LPC}$$
$$I_{HPC} = Ex_{18} - Ex_{19} + \dot{W}_{HPC} \tag{41}$$

where W_{LPC} and W_{HPC} are the compressor work of the low and high pressure compressors.

The performance criteria are:

$$\eta_{ex\,LPC} = \frac{Ex_{17} - Ex_{16}}{W_{LPC}}$$
$$\eta_{ex\,HPC} = \frac{Ex_{19} - Ex_{18}}{W_{HPC}} \tag{42}$$

3.6.4. Reboiler System (RS)

Reboiler systems offer the only technology available for removing NCGs from geothermal steam upstream of the turbine. Reboiler technology (vertical tube evaporator type) has been applied at the pilot level at the Geysers, California. During more than 1000 h of accumulated test time, the average H_2S removal efficiency obtained was 94% [27]. Later, the same reboiler system was tested at the Cerro Prieto Geothermal Field in Mexico. The nominal capacity of the equipment was 0.4 t/h of steam and after more than 200 test runs and 3000 operating hours, a mean value of 94% of gas removal efficiency was obtained [28].

A tray-type direct contact reboiler system was applied to 40 MW_e Latera Geothermal Power Plant in Italy where the NCG content is 3.5% at the wellhead. This is the first application to the geothermal industry in the World of the reboiler concept on a commercial scale. It was started up in early 1999 and abundant in 2003 because of the environmental problems [29].

A packed bed direct contact reboiler test process was applied to Kizildere GPP in Turkey. A 3-month test program with an accumulative test run time of approximately 260 hours was completed in January 1999, demonstrating the performance of a bench-scale packed bed direct contact reboiler. The test unit located at the KD 14 wellhead where the NCG content is at the design level (10%). During the tests CO_2 removal efficiency was obtained as 76.3 22.6% for a wide range of reboiler parameters [30].

In this study, a vertical tube evaporator reboiler is used (Figure 13). A vertical tube evaporator is a heat exchanger where the entering geothermal steam is condensed on the shell side. A small amount of the uncondensed steam flows out from the top of the shell side in a vent stream. The condensate is pumped to the top of the heat exchanger, where it enters the tube side and evaporates through the tubes. The clean steam leaving the reboiler contains a small amount of NCGs so that the capacity of steam ejector system is reduced. The rejection of NCGs to vent stream and steam/NCG weight ratio in vent gas are taken as 98% and 50%-50%, respectively. Reboiler system requires at least 330 kPa pressure drop between the separator and turbine inlet according to a study for KGPP [2-3, 31].

$$\dot{m}_{NCG,36} = 0.98 \times \dot{m}_{NCG,13b} \tag{43}$$

$$\dot{m}_{s,36} = \dot{m}_{NCG,36} \tag{44}$$

$$\dot{m}_{s,42} = (\dot{m}_{s,13b} - \dot{m}_{s,36}) \times 0.01 \tag{45}$$

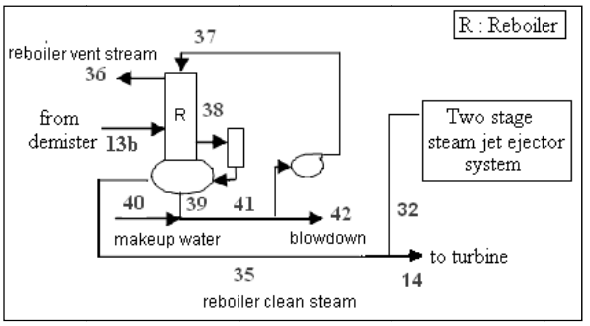

Figure 13. Flow diagram of reboiler system.

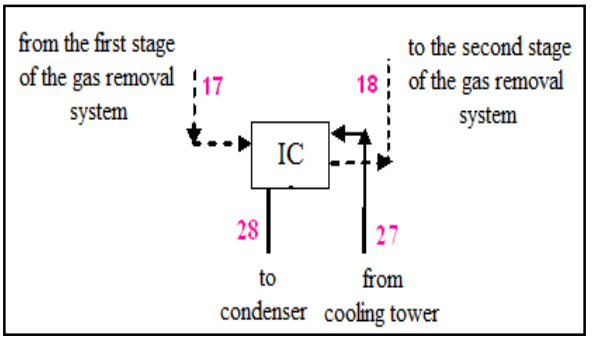

Figure 14. The inter-condenser flow diagram.

Exergy loss and exergetic efficiency are of the form:

$$I_{reboiler} = \dot{E}x_{13b} - \dot{E}x_{35} - \dot{E}x_{36} \tag{46}$$

$$\eta_{Ex,reboiler} = \frac{\dot{E}x_{35}}{\dot{E}x_{13b}} \tag{47}$$

3.6.5. Inter and after-Condensers

In a multi-stage turbine system, inter and after-condensers are typically used between the stages. By condensing the vapor prior to the next stage, the vapor load is reduced. This allows smaller NCG removal systems to be used, and reduces steam consumption. After-condenser can also be added to condense vapor from the final stage. Adding an after-condenser will not affect the overall system performance, but may ease disposal of vapor and act as a noise suppressor [18, 32].

Inter-Condenser (IC)

Flow diagram of inter-condenser is shown in Figure 14.

Inter-condenser heat load has the form:

$$\dot{Q}_{ic} = \dot{m}_{s,17} \times h_{s,17} + \dot{m}_{NCG,17} \times h_{NCG,17} - \dot{m}_{s,18} \times h_{s,18} - \dot{m}_{NCG,18} \times h_{NCG,18} - \left[(\dot{m}_{s,17} - \dot{m}_{s,18}) \right] \times h_{28} \tag{48}$$

The cooling water mass flowrate is:

$$\dot{m}_{cw,1} = \frac{\dot{Q}_{ic}}{(h_{28} - h_{27})} \tag{49}$$

Exergy loss and exergetic efficiency are of the form:

$$I_{ic} = \dot{E}x_{17} + \dot{E}x_{27} - \dot{E}x_{18} - \dot{E}x_{28} \tag{50}$$

$$\eta_{Ex,ic} = \frac{\dot{E}x_{17} + \dot{E}x_{27} - I_{ic}}{\dot{E}x_{17} + \dot{E}x_{27}} \tag{51}$$

After-Condenser (AC)

In Figure 15, flow diagram of after-condenser is presented. Similar to inter-condenser calculations, heat load is of the form:

$$\dot{Q}_{ac} = \dot{m}_{s,19} \times h_{s,19} + \dot{m}_{NCG,19} \times h_{NCG,19} - \dot{m}_{NCG,31} \times h_{NCG,31} - \dot{m}_{s,19} \times h_{25} \tag{52}$$

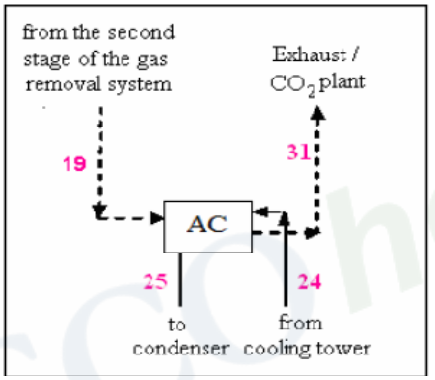

Figure 15. The after-condenser flow diagram.

Cooling water mass flowrate is:

$$\dot{m}_{cw,2} = \frac{\dot{Q}_{ac}}{(h_{25} - h_{24})} \tag{53}$$

Exergy loss and exergetic efficiency have the form:

$$I_{ac} = \dot{E}x_{19} + \dot{E}x_{24} - \dot{E}x_{31} - \dot{E}x_{25} \tag{54}$$

$$\eta_{Ex,ac} = \frac{\dot{E}x_{19} + \dot{E}x_{24} - I_{ac}}{\dot{E}x_{19} + \dot{E}x_{24}} \tag{55}$$

3.7. Water Circulation Pumps and Cooling Tower Fans

In a GPP, pumps play an important role in the cooling process. A representative single-flash GPP employing three water circulation pumps is considered, as shown in Figure 16.

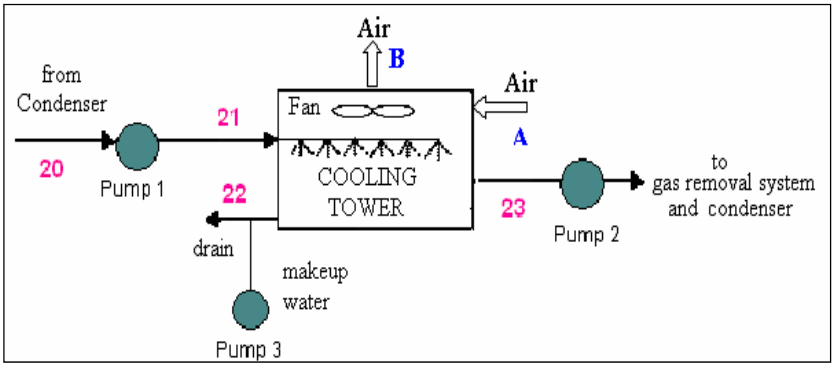

Figure 16. Water circulation pumps in the GPP.

- Pump1: from the condenser exit to the cooling tower inlet;
- Pump2: from the cooling tower exit to the condenser inlet;
- Pump3: for makeup water to the cooling tower inlet.

Make-up water must be added to the cycle to replace the water loss due to evaporation and air draft. To minimize the water carried away by the air, drift eliminators are installed in the wet cooling tower above the spray section [33].

The makeup water flowrate is calculated by

$$\dot{m}_{make\,up} = 1.22 \times Evaporation\ loss \tag{56}$$

The evaporation loss rate is 1-1.5% of the total circulating water flowrate. Blowdown is normally 20% of evaporation loss, but sometimes the value is similar to evaporation loss, depending upon the content of chemicals and various minerals, and the size of the plant. The drift loss is approximately 0.03% of the total circulating water flowrate [17].

$$Evaporation\ loss = \dot{m}_a \times (\omega_2 - \omega_1)$$

$$Drift\ and\ blowdown\ losses = 0.22 \times Evaporation\ loss \tag{57}$$

The following equations are used to calculate the power of water circulation pumps $\dot{W}_{pump}$:

$$\dot{W}_{pump} = \frac{\dot{V}_l \times \Delta P}{\eta_{pump}} \tag{58}$$

$$\dot{W}_{motor,\,pump} = \frac{\dot{W}_{pump}}{\eta_{motor,\,pump}} \tag{59}$$

Exergy loss and exergetic efficiency are of the form:

$$I_{pump} = \dot{E}x_{in} - \dot{E}x_{out} + \dot{W}_{pump} \tag{60}$$

$$\eta_{Ex,pump} = \frac{\dot{E}x_{in} - \dot{E}x_{out}}{\dot{W}_{pump}} \tag{61}$$

The air circulation in the cooling tower is provided by fans, and the power of the fans is determined in similar way with water circulation pumps by using Eqs. 58-61.

4. RESULTS

4.1. Mass and Energy Balances

A detailed mass and energy balance of a single-flash GPP is provided to compute the net power output, total auxiliary power, and specific steam consumption of the plant for various NCG removal system alternatives.

Table 2. Input parameters of the model

	Parameter		**Value**
Geothermal field	Flowrate (kg/s)	Wells	281.6
	Pressure (kPa)	Wells	1,800
		Wellhead	1,330
		Separator	460
	Temperature (°C)	Wells	204.7
	NCG fraction (%)	At the main separator exit	13
Power plant	Pressure (kPa)	Condenser	10
		Pressure drop between main separator exit and turbine inlet	10
		Pressure drop throughout the reboiler	320
		Pressure drop of fans/circulation pumps	0.1
Power plant	Pressure (kPa)	NCG removal system final stage discharge pressure	105
	Temperature (°C)	Water at cooling tower exit	29
	Efficiency (%)	Generator	90
		Compressor	75
		LRVP	40
		Fans/Circulation pumps	70
		Fans/Circulation pumps motor	85
Environmental	Pressure (kPa)	Dead state	95
	Temperature (°C)	Dead state	16
	Relative humidity (%)	Dead state	65

Table 3. Main results of the mass and energy balance of the plant with Kizildere operational data

NCG Removal System		**CS**	**SJES**	**HS**	**RS**
Separator Pressure (kPa)		460	460	460	460
Condenser Pressure (kPa)		10	10	10	10
Auxiliary Power (kW)	Compressor /LRVP	1262		1299	
	Steam Jet Ejector *		6666	3038	180
	Water Circulation Pumps	346	372.4	360.3	192
	Cooling Tower Fans	86.3	91.5	89.8	47.2
	Other	150	150	150	150
	TOTAL	1844	7279	4936	569.2
Net Power Output (kW)		10235	5466	7447	5667

*Consumed motive flow rate is converted into power in kW.

Kizildere GPP-Turkey operational data and main assumptions are listed in Table 2. The main results of the mass and energy balance of the plant are presented in Table 3.

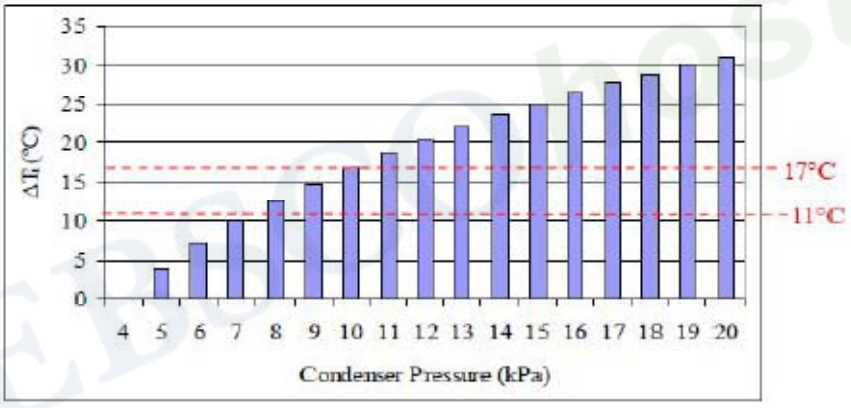

Figure 17. Condenser pressure vs. ΔT_i.

4.1.1. Condenser and Separator Pressures

The temperature regime in the condenser is one of the limiting factors for determining of condenser pressure. The difference between saturated temperature and cooling water inlet temperature (ΔT_i) should be between about 11 and 17°C [25]. Condenser pressure range is taken as 4-20 kPa to check the ΔT_i, and the results are illustrated in Figure 17. The Figure indicates that recommended temperature range falls into 8-10 kPa condenser pressure range. Therefore, the range for condenser pressure is taken as 8-10 kPa for simulation.

Net power output of the plant is calculated for condenser and separator pressures of 8-10 kPa and 100-1000 kPa, respectively, to evaluate the effects of condenser and separator pressures on thermodynamic performance of the plant. The net power output versus separator pressures is shown in Figure 18 at 13% NCG fraction.

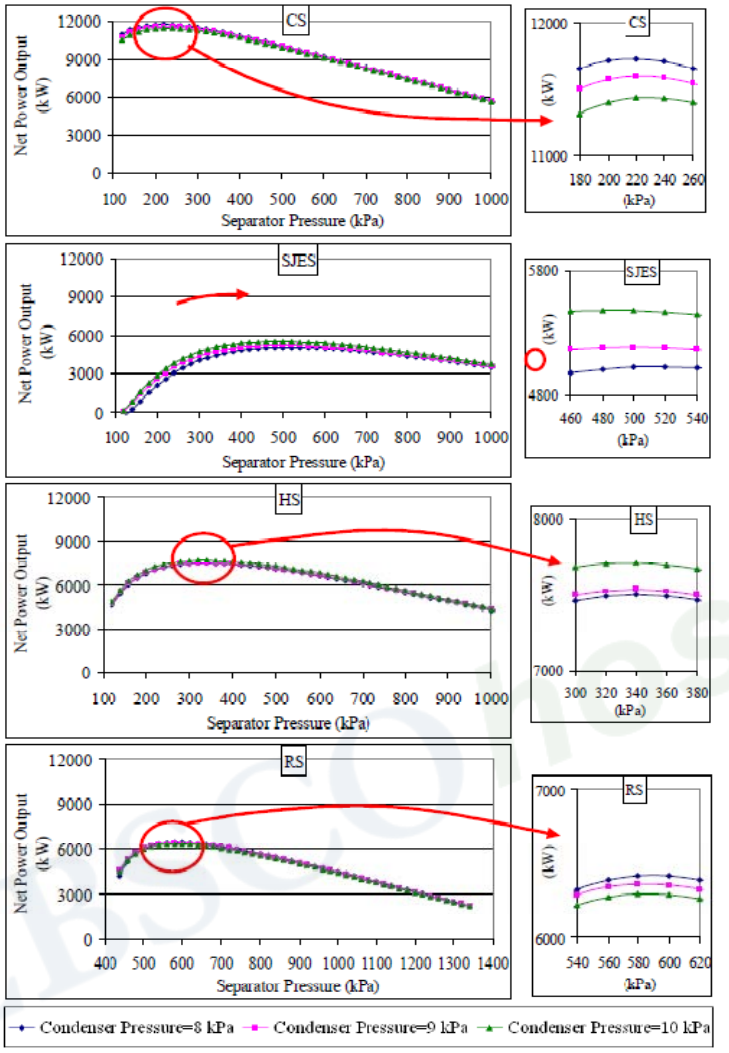

Figure 18. Net power output of the plant for various separator and condenser pressures.

Table 4. Main results of mass and energy balance of the plant at optimum separator pressures

NCG Removal System		**CS**	**SJES**	**HS**	**RS**
Optimum Separator Pressure (kPa)		220	500	340	580
Condenser Pressure (kPa)		10	10	10	10
Auxiliary Power (kW)	Compressor /LRVP	1749		1518	
	Steam Jet Ejector *		6239	3645	370
	Water Circulation Pumps	486	353	424	252
	Cooling Tower Fans	121	87	106	62
	Other	150	150	150	150
	TOTAL	2506	6829	5843	834
Net Power Output (kW)		11436	5476	7712	6294

* Consumed motive flow rate is converted into power in kW.

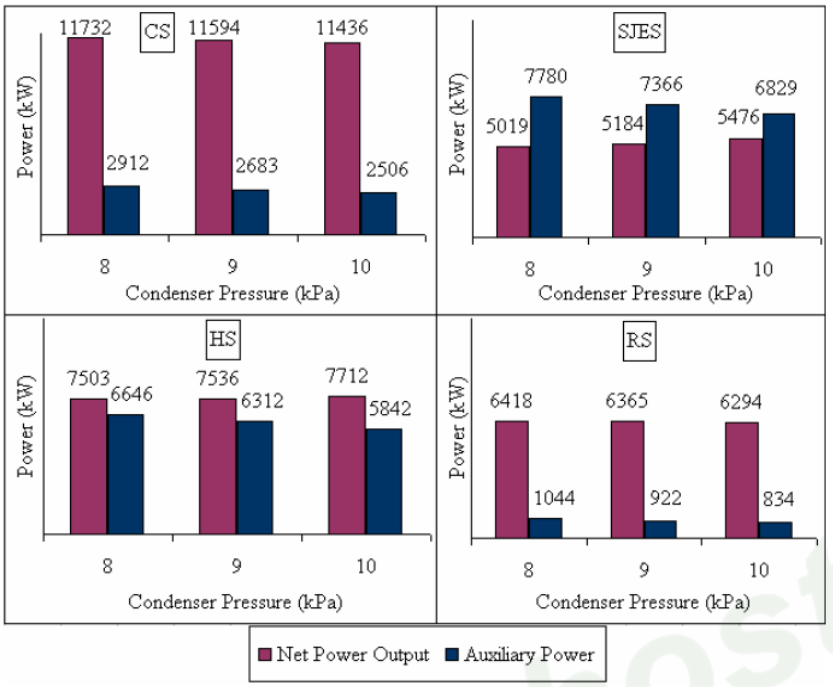

Figure 19. Net power output and total auxiliary power of the plant for various condenser pressures for optimum separator pressures.

Figure 18 indicates that increasing separator pressure increases the net power output up to a peak value, which corresponds to optimum separator pressure. Further increase in separator pressure shows a dramatic decrease in net power production caused by a consequent decrease in steam flowrate. Optimum separator pressures obtained from Figure 18 are 220 kPa for CS, 500 kPa for SJES, 340 kPa for HS, and 580 kPa for RS at 13% NCG fraction.

To compare the thermodynamic performance of the plant with operational and optimum separator pressures, the net power output and auxiliary power are calculated at optimum separator pressures of each NCG removal system, and the results, summarized in Table 4, show that the net power outputs increase between 0.2-11.7% by using optimum separator pressures.

The effect of condenser pressure on the net power output and the auxiliary power is evaluated for a range of 8-10 kPa (Figure 19). Figure 19 exhibits that increasing condenser pressure causes an increase in the net power output for SJES and HS while a decrease encountered for CS and RS. On the other hand, increasing condenser pressure decreases the auxiliary power requirement as well as the O&M costs. As an example, changing the condenser pressure from 8 kPa to 10 kPa results in a 2.5% (296 kW) decrease in net power output of CS, and a 14% (406 kW) decrease in auxiliary power. Because a higher auxiliary power allows for a larger equipment size and a higher cost, the 10 kPa condenser pressure is selected as optimum pressure with the lowest auxiliary power.

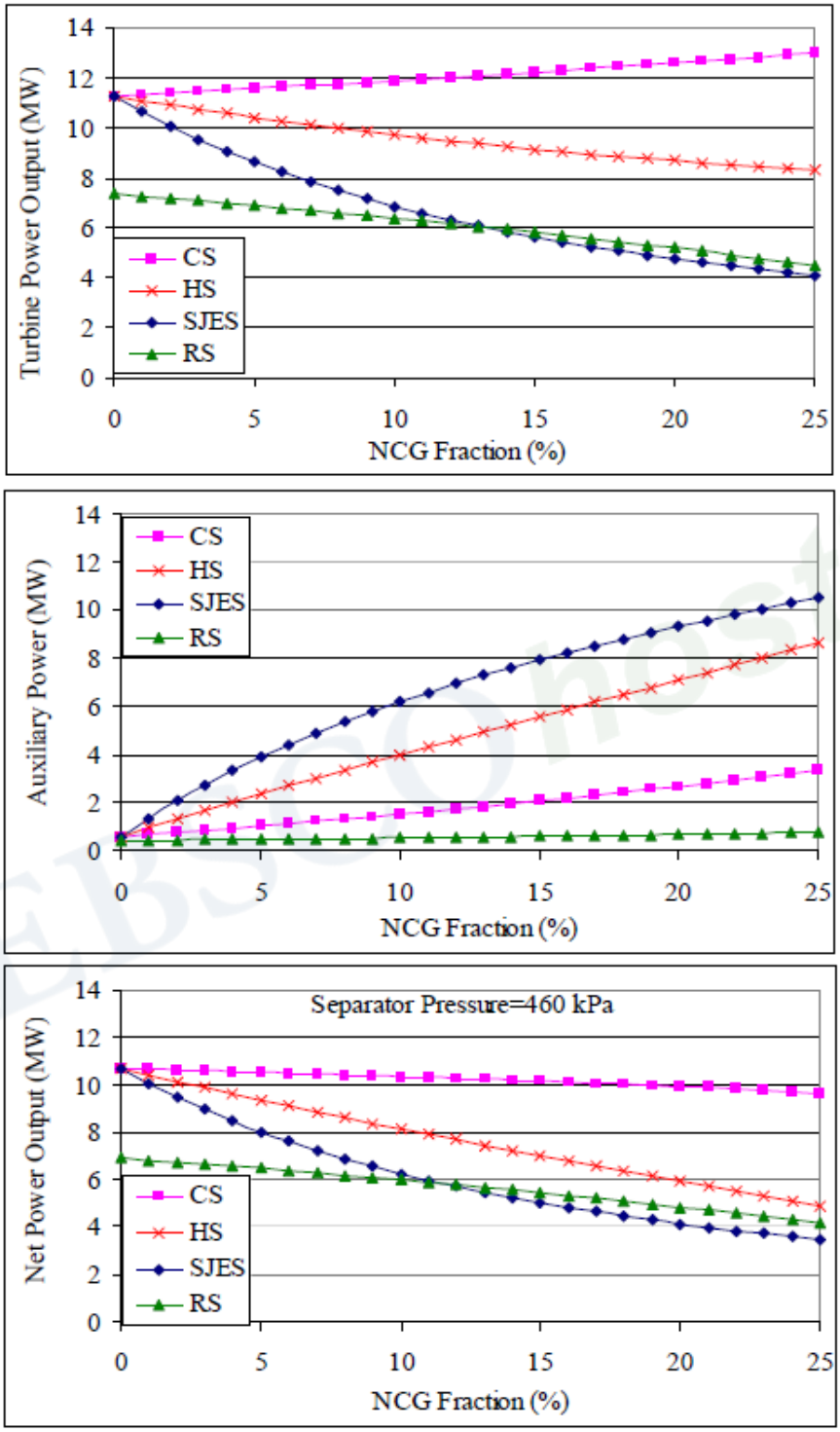

Figure 20. Turbine power output, net power output and auxiliary power of the plant vs. NCG fraction.

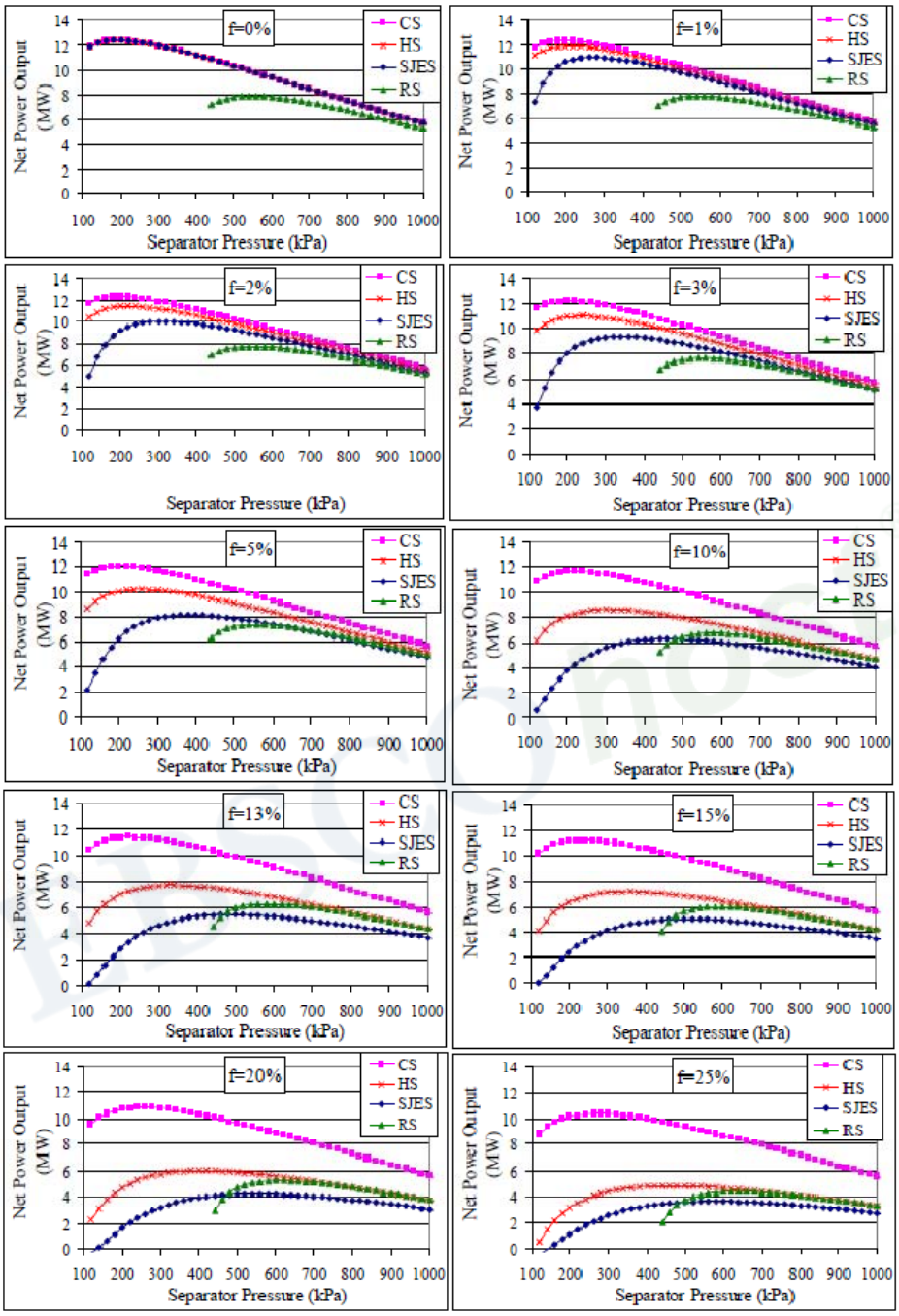

Figure 21. Separator pressure vs net power output of the plant for various NCG fractions.

4.1.2. NCG Fraction

The effect of NCG fraction on the turbine power output, auxiliary power and net power output is plotted in Figure 20 for a 0-25% range of NCG fraction. The Figure indicates that the auxiliary power increases and the net power output decreases with increasing NCG fraction. An increase in NCG fraction (1%) causes a net power output loss of 0.4% for CS,

2.2% for HS, 2.5% for RS, and 2.7% for SJES. Especially, SJES has a dramatic decrease in net power output by NCG fraction. On the other hand, it is interesting to observe that the turbine power output of CS increases with increasing NCG fraction. The reason for that is the increase in steam quality at the separator by the existence of NCG in the steam. Therefore, separator pressure has vital importance for maximizing the net power output. Figure 21 shows the separator pressure versus the net power output of the plant for various NCG fractions (0-25% by weight of steam) at 10 kPa condenser pressure.

Figure 21 shows that each NCG removal option exhibits the same behavior for a zero NCG fraction except RS. This is because RS requires at least 330 kPa pressure drop between the separator and turbine inlet, while the other NCG removal systems require 10 kPa. Figure 21 shows that the optimum separator pressures, which maximize the net power output, change with the NCG fraction.

4.2. Exergy Balance

For given data of KGPP and the assumptions made, an exergy analysis is conducted to evaluate four different conventional gas removal options under a range of NCG fraction (0-25%). Representing the operational conditions of KGPP, NCG content and turbine inlet pressure are taken as 13% and 450 kPa, respectively. Exergy distribution throughout the plant for each gas removal option is evaluated and an example is given in Figure 22 for compressor gas removal option. Figure 22 exhibits that production wells provide a total exergy of 52968 kW at the wellhead. Major exergy destruction locations are separator (steam+liquid exits), turbine and generator, cooling tower, condenser and gas removal system.

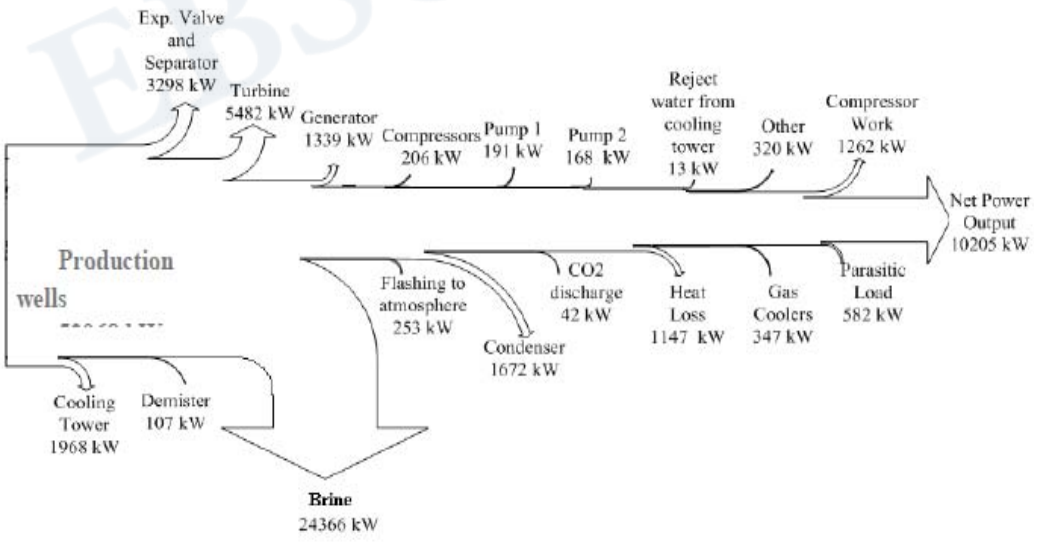

Figure 22. Exergy flow chart of the geothermal power plant with compressor gas removal system.

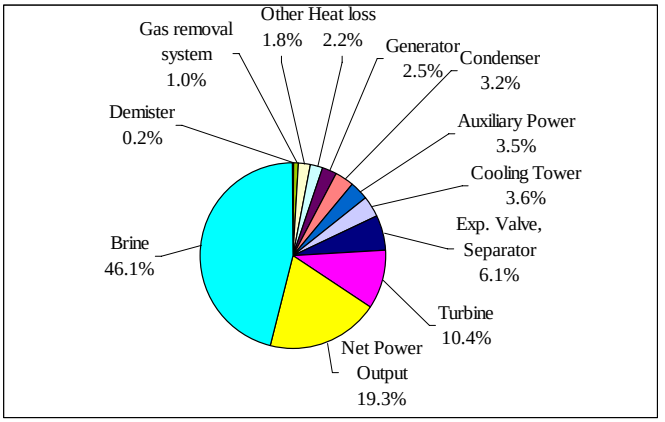

Figure 23. Overall exergy balance of CS.

Overall exergy balance of the system is shown in Figure 23.

As the geothermal fluid is flashed into steam and brine in the separators, a total exergy of 3298 kW is destroyed during the separation process itself, and this loss corresponds to 6.2% of the total exergy input.

The remaining brine at relatively low temperature and pressure is first sent to the silencer and then is re-injected or directed to the other direct use applications. A total exergy of 24366 kW, which amounts 46% of the total exergy input, is corresponding to brine. The demister is located between separator and turbine. Assuming a 10 kPa pressure drop between separator and turbine, the exergy loss of the demister is calculated as 107 kW and 1% of the steam is flashed in the demister wasting 253 kW of exergy. The exergy loss of the turbine is 5482 kW, which amounts as 10.3% of the total exergy input. The exergy further destroyed in the generator during the conversion of the mechanical shaft work to the electrical energy. This accounts for 2.5% of the total exergy destruction. Cooling tower and condenser are the other vital components with 1968 and 1672 kW exergy destruction, respectively. The pipe between the condenser exit and cooling tower inlet is assumed to have 3°C temperature drop. Therefore, the exergy destruction with heat loss is calculated as 1147 kW.

For the gas removal system, the exergy loss is 206 kW for the compressor and 347 kW for gas coolers. The total exergy loss of the gas removal system is 554 kW, which is 1% of the total exergy input. A further usage of exergy output is consumed by internal devices such as auxiliaries, pumps, fans and control systems. This parasitic load is calculated as 582 kW and compressor work is 1262 kW. The total exergy destruction of the plant is 42763 kW, which is 80.7% of the total exergy input. The remaining 10205 kW leaves the plant as the net power output. Exergy loss distribution of the plant components for each gas removal option are summarised in Table 5 for 450 kPa turbine inlet, 10 kPa condenser pressures and 13% NCG fraction.

Figure 24 exhibits the overall exergetic efficiency of gas removal systems depending on NCG fraction at operational turbine inlet pressure of the KGPP. Among the gas removal options, the compressor system accounts the highest overall exergetic efficiency. Reboiler system is the worst option for low NCG fractions, for high NCG fractions it becomes more efficient than steam jet ejector system.

Table 5. Exergy losses of the NCG removal systems

Components	CS		SJES		HS		RS	
	(kW)	(%)	(kW)	(%)	(kW)	(%)	(kW)	(%)
Exergy losses of main equipment	38524	72.8	34447	65.1	36679	69.3	40353	76.3
Expansion valve+Separator	3221	6.1	3221	6.1	3221	6.1	1174	2.2
Brine	24384	46.1	24384	46.1	24384	46.1	33339	63.0
Demister	107	0.2	107	0.2	107	0.2	41	0.1
Turbine	5496	10.4	2767	5.2	4252	8.0	2941	5.6
Generator	1342	2.5	676	1.3	1038	2.0	673	1.3
Condenser	1707	3.2	859	1.6	1321	2.5	930	1.8
Cooling tower	1924	3.6	2063	3.9	1999	3.8	1065	2.0
Pump1	176	0.3	189	0.4	183	0.3	97	0.2
Pump2	168	0.3	181	0.3	175	0.3	93	0.2
Reject to the atmosphere or river	309	0.6	307	0.6	308	0.6	3236	6.1
Rejection from cooling water	14	0.0	12	0.0	0.0	15	8	0.0
Flashing to the atmosphere	253	0.5	253	0.5	0.5	278	184	0.3
CO_2 discharge	42	0.1	42	0.1	0.1	49	1	0.0
Vent from reboiler							3043	5.8
Heat loss	1147	2.2	1233	2.3	1194	2.3	637	1.2
Pipe	1147	2.2	1233	2.3	1194	2.3	637	1.2
Other	300	0.6	1683	3.2	328	0.6	907	1.7
NCG removal system	556	1.0	9165	17.3	5059	9.6	1735	3.3
Compressors/SJES	206	0.4	3623	6.8	2426	4.6	93	0.2
LRVP/Reboiler					540	1.0	1501	2.8
Inter and after condensers	349	0.7	5542	10.5	2093	4.0	142	0.3
Auxiliary power	1844	3.5	614	1.2	1899	3.6	389	0.7
Parasitic load (pumps, fan etc.)	582	1.1	614	1.2	600	1.1	389	0.7
Compressor work/LRVP	1262	2.4			1299	2.5		

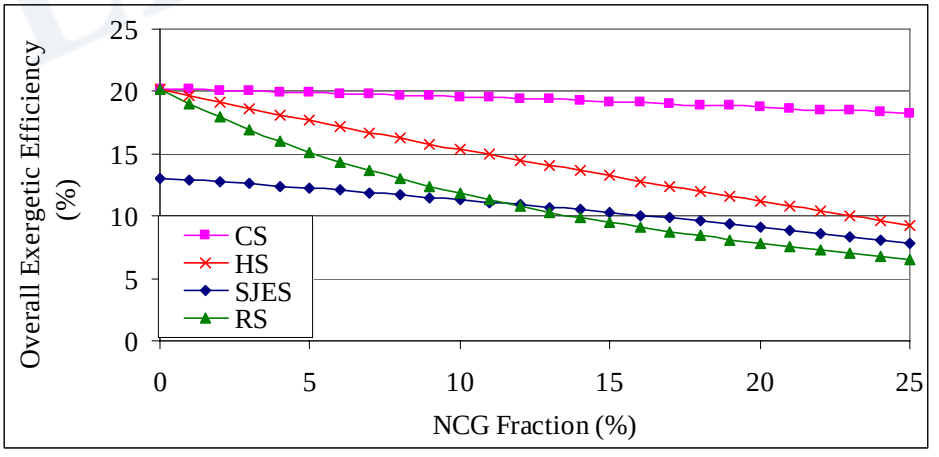

Figure 24. Overall exergetic efficiency of gas removal systems depending on NCG fraction at operational turbine inle pressure of KGPP.

Table 6. Comparison of exergetic efficiencies of the main components of the plant for different gas removal options at13% NCG fraction and 450 kPa turbine inlet pressure.

Component	Exergetic Efficiency (%)			
	CS	SJES	HS	RS
Expansion valve+separator	47.8	47.8	47.8	34.8
Turbine-generator	63.9	63.9	63.9	62.6
Condenser	76	87	81.	78.

Table 6 lists the exergetic efficiencies of main component of the plant for different gas removal options at operational conditions of KGPP (13% NCG fraction and 450 kPa turbine inlet pressure). Under the given conditions, turbine-generator and cooling tower exhibit a similar performance, while expansion valve+separator and condenser are more sensitive to gas removal system change.

Production wells provide a total exergy of 52915 kW at the wellhead. Major exergy destructions occur due to the separation of steam from geothermal fluid, the discharge of the geothermal fluid from the separator, turbine and generator, cooling tower, condenser and NCG removal system.

CONCLUSIONS

A deterministic and static model of single-flash GPPs is developed and a code written in EES software is employed to examine the effects of NCGs and gas removal systems on GPP performance. The modeled NCG removal system alternatives include compressor system (CS), steam jet ejector system (SJES), hybrid (steam jet ejector and LRVP) system (HS), and reboiler system (RS). The model is firstly run with Kizildere GPP input parameters. Then plant is simulated based on various input variables, such as separator pressure, condenser pressure and NCG fraction.

The main conclusions derived from the analysis are:

1. NCG fraction is the most influencing factor on GPP performance.The net power output and overall exergetic efficiency of a single-flash GPP is decreased by;

    - 0.4% for CS;
    - 2.2% for HS;
    - 2.5% for RS, and;
    - 2.7% for SJES by a 1% increase in NCG fraction.

2. The compressor system is the most efficient and robust system where the influence of the NCG fraction is limited. On the other hand, steam jet ejectors are highly affected by increasing NCG fraction since motive steam flowrate to the steam jet ejectors is directly related to NCG fraction. Thus they exhibit as the worst case. Hybrid system is responded late to the change in NCG fraction because the LRVP is more efficient since its performance lies between compressors and steam jet ejectors.
3. The optimum separator pressure, corresponding to the maximum net power output, is highest for SJES and lowest for CS at the same NCG fraction. Net power output of the plant decreases with increasing separator pressure with a decrease in steam flowrate feeding the turbine. This makes the situation more dramatic for steam jet ejectors in a feasibility study. To increase the power output, steam flowrate should be increased by drilling more wells, which leads to the higher cost of field development.
4. Thermodynamic performance of a single-flash plant can be improved by 0.2-11.7% with the optimum separator and condenser pressures. GPPs should be operated in design conditions to generate optimum net power.
5. While the pressure drop between the separator and turbine inlet is as low as 10 kPa for the first three options, 330 kPa should be maintained for reboiler system. Therefore, separator pressure is the highest for reboiler option at the same NCG fraction. Increase in separator pressure results in a decrease in steam flowrate thus yields a lower power output per unit of steam feeding the turbine.
6. An examination of the exergy destruction throughout the plant reveals that the largest exergy destruction occurs from the brine discharge after flashing processes in the separators. For operational turbine inlet pressure (450 kPa) and 13% NCG fraction, it accounts for 63% for reboiler system and 46.1% for the other systems of the total exergy input. Therefore, alternative cycles (such as combined cycle, double flash, binary plant etc.) should be considered to save considerable amount of the exergy loss from brine discharge.
7. Exergy analyses indicate that the exergetic efficiency is 61.5% for the cooling tower and around 63.9% for turbine-generator couple for 450 kPa turbine inlet pressure and 13% NCG fraction. The results show that cooling tower and turbine-generator couple are the major exergy consumers and they have the largest improvement potential.
8. According to the results of the exergy analyses, while the compressor system has the highest overall exergetic efficiency of 19.3%, steam jet ejector system has the lowest with 10.3% for operational condition of KGPP. The overall exergetic efficiencies of hybrid and reboiler gas removal systems are 14% and 10.7%, respectively.

REFERENCES

[1] Hall, N. R.: Gas extraction system in M.G. Dunstall (eds.) Geothermal Utilisation Engineering Lecture Notes, Geothermal Institute, The University of Auckland, New Zealand (1996).

[2] Coury, G., Guillen, H. V. and Cruz, D. H.: Geothermal noncondensable gas removal from turbine inlet steam. Proceedings 31st Intersociety 3 Energy Conversion Engineering Conference, (1996).

[3] Vorum M. and Fritzler E.A.: Comparative Analysis of Alternative Means for Removing Non-Condensable Gases From Flashed-Steam Geothermal Power Plants. NREL Report SR-550-28329, Colorado, The USA (2000).

[4] Dincer, I. and Rosen M.A.: Thermodynamic aspects of renewables and sustainable development, *Renewable and Sustainable Energy Reviews*, 9, (2005), 169-189.

[5] Rosen M.A. and Dincer, I.: Effect of variying dead-state properties on energy and exergy analyses of thermal systems. *International Journal of Thermal Sciences*, 43, (2004), 121-133.

[6] Ozturk, H.K., Atalay, O., Yilanci, A. and Hepbasli, A.: Energy and exergy analysis of kizildere geothermal power plant, Turkey, *Energy Sources*, Vol. 23, (2006), 1415–1424.

[7] Khalifa, H.E. and Michaelides, E.: The Effect of Noncondensable Gases on the Performance of Geothermal Steam Power Systems, US Department of Energy Report, Report No. CATMEC/28, Rhode Island, The USA (1978).

[8] Michaelides, E.E.: Separation of noncondensables in geothermal installations by means of primary flashing, *Transactions Geothermal Resources Council*, Vol. 4, (1980), 515–518.

[9] Awerbuch L., Van Der Mast, V.C. and Soo-Hoo, R.: Review of upstream reboiler concept, *Transactions Geothermal Resources Council*, Vol. 8 (1984), 21-26.

[10] Gunerhan (Gokcen), G.: Theoretical and Experimental Investigations on Condensation/Boiling Modelled Heat Exchangers (Reboilers) Designed for Removal of Non-Condensable Gases from Geothermal Steam, PhD Thesis, Ege University-İzmir-Turkey (2000) (in Turkish).

[11] Allegrini, G., Sabatelli, F. and Cozzini, M.: Thermodynamic analysis of the optimum exploitation of a water-dominated geothermal field with high gas content. Seminar on New Developments in Geothermal Energy, Committee on Electric Power, Economic Commission on Europe, United Nations, Ankara, (1989).

[12] Sabatelli, F. and Mannari, M.: Latera development update. *CD Transactions World Geothermal Congress*, Florence, Italy, Vol. 3, (1995), 1785-1789.

[13] Yildirim, E.D., and Gokcen, G.: Exergy analysis and performance evaluation of kizildere geothermal power plant, Turkey, *International Journal of Exergy*, Vol. 1, (2004), 316–333.

[14] Hankin, J.W., Cochrane, G. F. and Van der Mast, V. C.: Geothermal Power Plant Design for Steam with High Noncondensable Gas. *Transactions Geothermal Resources Council*,Vol. 8 (1984), 65-70.

[15] Gokcen G., Yildirim N.: Effect of Non-Condensable Gases on geothermal power plant performance. Case study: Kizildere Geothermal Power Plant-Turkey. *International Journal of Exergy*, 5, (2008), 684-695.

[16] F-Chart: Engineering Equation Solver (EES) software, website of F-Chart, *http://fchart.com*, (2009).

[17] Siregar, P.H.H.: Optimization of Electrical Power Production Process for The Sibayak Geothermal Field, Indonesia, UNU Geothermal Training Programme Report, Report No. 16, Reykjavik, Iceland, (2004).

[18] Swandaru, R. B.: Thermodynamic Analysis of Preliminary Design of Power Plant Unit I Patuha, West Java, Indonesia, UNU Geothermal Training Programme Report, Report No:7, Reykjavik, Iceland (2006).

[19] Dunya, H.: Data of KGPP (2008) (personal comm.).
[20] DiPippo, R.: The Effect of Expansion-Ratio Limitations on Positive-Displacement, Total-Flow Geothermal Power Systems, *Transactions Geothermal Resources Council*, Vol. 6, (1982) 343-346.
[21] TTMD: Meteorological Data of Turkey, Technical Publication of Turkish Society of HVAC and Sanitary Engineers, (2000) (in Turkish).
[22] Yildirim Ozcan, N., and Gokcen G.: Energy Analysis of Removing Non-Condensable Gases from Single-Flash Geothermal Power Plants, Proceedings, 4th International Exergy, Energy and Environment Symposium, AUS, Sharjah, UAE (2009).
[23] Kwambai, C.B.: Exergy Analysis of Olkaria I Power Plant, Kenya, *UNU Geothermal Training Programme Report*, Report No. 5, Reykjavik, Iceland (2005).
[24] DiPippo, R.: Geothermal Power Plants Principles, Applications and Case Studies, *Elsevier Science*, ISBN-10: 1856174743, Oxford, UK (2005).
[25] El-Wakil, M,M: *Geothermal Plant Technology*, McGraw-Hill Inc, NewYork, 859 pp (1984).
[26] Moghaddam, A.R.: A conceptual Design of A Geothermal Combined Cycle and Comparison with a Single-Flash Power Plant for Well NWS-4, Sabalan, Iran, Report of the United Nations University Geothermal Training Programme, *Report No:18*, pp:391-428, Reykjavik, Iceland (2006).
[27] Coury, G.E. and Associates.: Upstream H2S removal from geothermal steam, *Technical Report EPRI*, AP-2100, 3.1-3.23. 1981.
[28] Angulo, R., Lam, L., Gamiño, H., Jiménez, H. and Hughes, E.E.: Developments in geothermal energy in Mexico- part six. Evaluation of a process to remove non-condensable gases from flashed geothermal steam upstream of a power plant. *Journal of Heat Recovery Systems*, Vol. 6 (1986), 295-303.
[29] Bertani, R.: World Geothermal Power Generation 2001-2005, Bulletin Geothermal Resources Council, May / June (2006).
[30] Gunerhan (Gokcen), G. and Coury, G.: Upstream reboiler design and test for removal of noncondensable gases from geothermal steam for Kizildere geothermal power plant, Turkey. *CD Transactions World Geothermal Congress 2000*, Kyushu - Tohoku, Japan, Vol. 5 (2000), 3173-3178.
[31] Gunerhan (Gokcen), G.: An Upstream Re-Boiler Design for Removal of NCGs from Geothermal Steam. Geothermal Institute Report, Report No: 96.10, University of Auckland, New Zealand (1996).
[32] Birgenheier, D.B., Butzbach, T.L., Bolt, D.E., Bhatnagar, R.K., Ojala, R.E. and Aglitz, J.: Designing Steam-Jet Vacuum Systems, Chemical Engineering, *www.graham-mfg.com/downloads/23.pdf.* (accessed 2008) (1993).
[33] Cengel, Y., Boles, M.A.: Thermodynamics: An Engineering Approach 6th Ed.; McGraw-Hill (2006).